Supplementary Information

Concomitant Induction to Few-layer and 1T-rich Two-dimension MoS_2 by Rigid Segment-containing Polysulfide as Sulfur Source and in situ Intercalator

Yijuan Wang, [a,b] Jianzhi Wang, [a] Jie Liu, [a] Zhuangwei Xiao, [a] Yanan Xue, [a] and Faquan Yu *[a]

a. Key Laboratory for Green Chemical Process of Ministry of Education，Hubei Key Laboratory for Novel Reactor and Green Chemistry Technology and School of Chemical Engineering and Pharmacy, Wuhan Institute of Technology, Wuhan 430205, P. R. China. E-mail: fyu@wit.edu.cn, fyuwucn@gmail.com
b. School of Medicine, Wuhan College of Arts & Science, Wuhan 430345, P. R. China

Experimental

Reagent

Sulfur sublimed (S), Sulfuric acid (H_2SO_4), N,N-dimethylformamidel (DMF, C_3H_7NO), commercial molybdenum disulfide (MoS_2) and thiourea (CH_4N_2S) were purchased from Sinopharm Chemical Reagents Co., Ltd. 1,3-Diisopropenylbenzene ($C_{12}H_{14}$, DIB) and molybdenum pentachloride ($MoCl_5$) were bought from Aladdin reagent (Shanghai) Co., Ltd. Nafion (5 wt%) was purchased from Dupont China Holding Co., Ltd. Commercial Pt/C catalyst (20 wt%) was purchased from Shanghai Macklin Biocheimal Co., Ltd. All chemical reagents were of analytical grade and used without any further purification. Water was purified to >18.2 MΩ•cm resistance and <10 ppb total organic content using a Barnstead Nanopure system.

Preparation of poly (sulfur-random-1, 3-diisopropenylbenzene) (poly(S-r-DIB))

Polysulfide called poly(S-r-DIB) was prepared by the ring opening polymerization via inverse vulcanization technique following the literature procedure.[1,2] A glass bottle (25ml) containing sulfur sublimed (4.50 g) and a small magnetic stir bar, was heated to T=185℃ in dimethyl silicone oil bath. When a clear yellow molten sulfur was formed, DIB (0.5 g) was rapidly added to the molten medium using a syringe under continuous agitation. After about 10 minutes under 185 ℃, the mixture turned into a red vitrification medium, then poly(S-r-DIB) was obtained. The poly(S-r-DIB) applied here contained 10 wt% DIB and 90 wt% elemental sulfur in the polymerization, which

corresponded to 44 S units per DIB unit on average according to the reported method.[1]

Synthesis of MoS_2 nanosheets

Above prepared poly(S-r-DIB) (0.4347g) was scraped by a metal spatula and dissolved in DMF (50 ml) in a water bath. $MoCl_5$ (1.366 g) was rapidly weighed and dissolved in DMF (40 ml), and prepared for 0.125 mol L^{-1} solution. The prepared poly(S-r-DIB) solution (10 ml) and $MoCl_5$ solution (4 ml) were mixed with DMF (16 ml) and transferred into a 50ml Teflon-lined stainless-steel autoclave. The autoclave was heated at 185°C for 15 h, and the black sediment was obtained after 7500r/min centrifugation for 20min. After washing with DMF and water for two times respectively, MoS_2 nanosheets were be obtained by freeze-drying, denoted as MoS_2-p. For comparison, MoS_2-m nanosheets were synthesized in a similar procedure with sulfur (0.08g) sublimed as the sulfur source in place of sulfur. Sulfur sublimed have a cyclo-octasulfur structure and can be considered as a short-chain molecule.[3] MoS_2-s nanosheets were also obtained in a similar procedure with thiourea as the sulfur source in place of polysulfide.

Electrochemical Measurements

All electrochemical measurements were explored using a CHI 760E Electrochemical Workstation (CHI Instruments, China) with a classical three-electrode glass cell. A saturated calomel electrode (SCE) was used as a reference electrode, and a graphite rod was applied as a counter electrode. The working electrode was prepared by the glassy carbon (GC) covered with a thin catalyst film. 4 mg of catalyst, 1 mg of conductive carbon black and 10 μl of Nafion solution (5 wt %) were dispersed in 1ml of water/ethanol mixture (1:1, v/v) to form a homogeneous catalyst ink assisted by ultrasound for 1 h. Then, the catalyst ink (5 μl) was dropped on a polished GC electrode with a 3 mm diameter and dried at room temperature. The loading amount of the catalyst is 0.28 mg cm^{-2}.

Prior to measurement, H_2SO_4 (0.5 $_M$) aqueous solution was degassed for 30 min by nitrogen to remove dissolved oxygen. All the electrochemical performance was tested at 25°C. The SCE reference electrode was calibrated with respect to a reversible

hydrogen electrode (RHE). In 0.5 $_{M}$ H_2SO_4, E (RHE) =E (SCE) +0.273. Linear sweep voltammetry (LSV) was investigated at a scan rate of 2 mV s^{-1} for the polarization curves after the resistance test, and the infrared (IR) compensation was applied using the CHI software. The Electrochemical impedance spectroscopy (EIS) analyses were performed in the frequency range of 10 kHz to 0.01 Hz under the amplitude of 5 mV. The Nyquist plots were tested under the voltage at the overpotential -150 mV versus RHE in 0.5 $_{M}$ H_2SO_4.Electrochemical double layer capacitance (C_{dl}) of each synthesized material was measured by CV in non-faradaic region from 0.1 to 0.2 V versus RHE with different scan rates (20, 40, 60, 80, 100, 120, 140 and 160 mV s^{-1}) to estimate the effective electrode surface area. Through a plot of different scan rate, the slope of the fitting line was found to be equal-to-twice the C_{dl}. The electrochemical stability was performed using CV sweeps at 100 mV s^{-1} between -0.4 and 0.1 V versus RHE for 5000 cycles in 0.5 $_{M}$ H_2SO_4 at 25°C. The long-term durability was measured using chronopotentiometry at a constant current density of 10 mA cm^{-2} in 0.5 $_{M}$ H_2SO_4 electrolyte. The after long-term chronopotentiometry test samples was obtained by dropping onto carbon paper to HER electrochemical stability test and then by ultrasound and drying.

Material Characterization

The structure and morphology were investigated by Field emission scanning electron microscopy (FESEM, GeminiSEM 300), and Transmission electron microscopy (TEM, Titan G260-300). The crystal phases of samples were tested by X-ray powder diffraction (XRD, Shimadzu XRD-6100) with high-intensity Cu Kα radiation. The X-ray photoelectron spectrometer (XPS) was recorded on Thermo Fisher ESCALAB Xi using an Al Kα as X-ray source, the banding energies of Mo, S, and O were referred to the C 1s peak at 284.8 eV. Raman spectra were obtained on a Laser confocal Microscopy Raman Spectrometer (DXR RAMAN MICROSCOPE) using 532 nm Raman spectroscopy. FT-IR test was carried on PerkinElmer FT-IR Spectrometer. Contact angles were measured using a contact angle goniometer (DSA100).

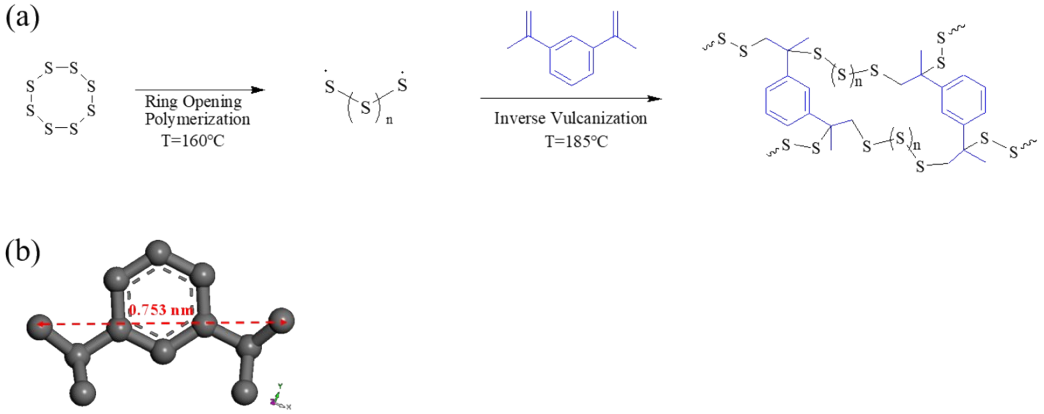

Scheme S1. (a) Schematic for the synthesis process of poly(S-r-DIB). (b) The maximum length of 1, 3-diisopropylbenzene structure in the poly(S-r-DIB) (measured by Materials Studio software).

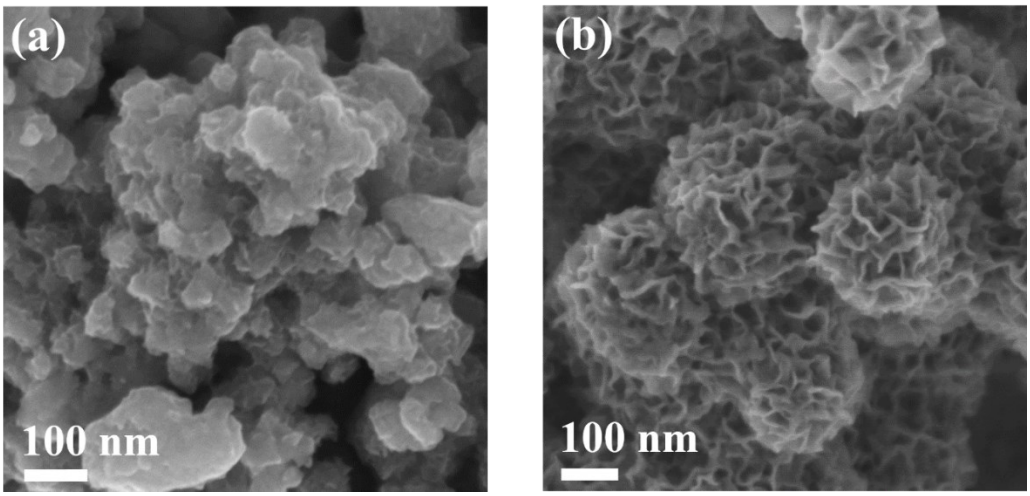

Fig. S1 SEM images of (a) MoS_2-m and (b) MoS_2-s.

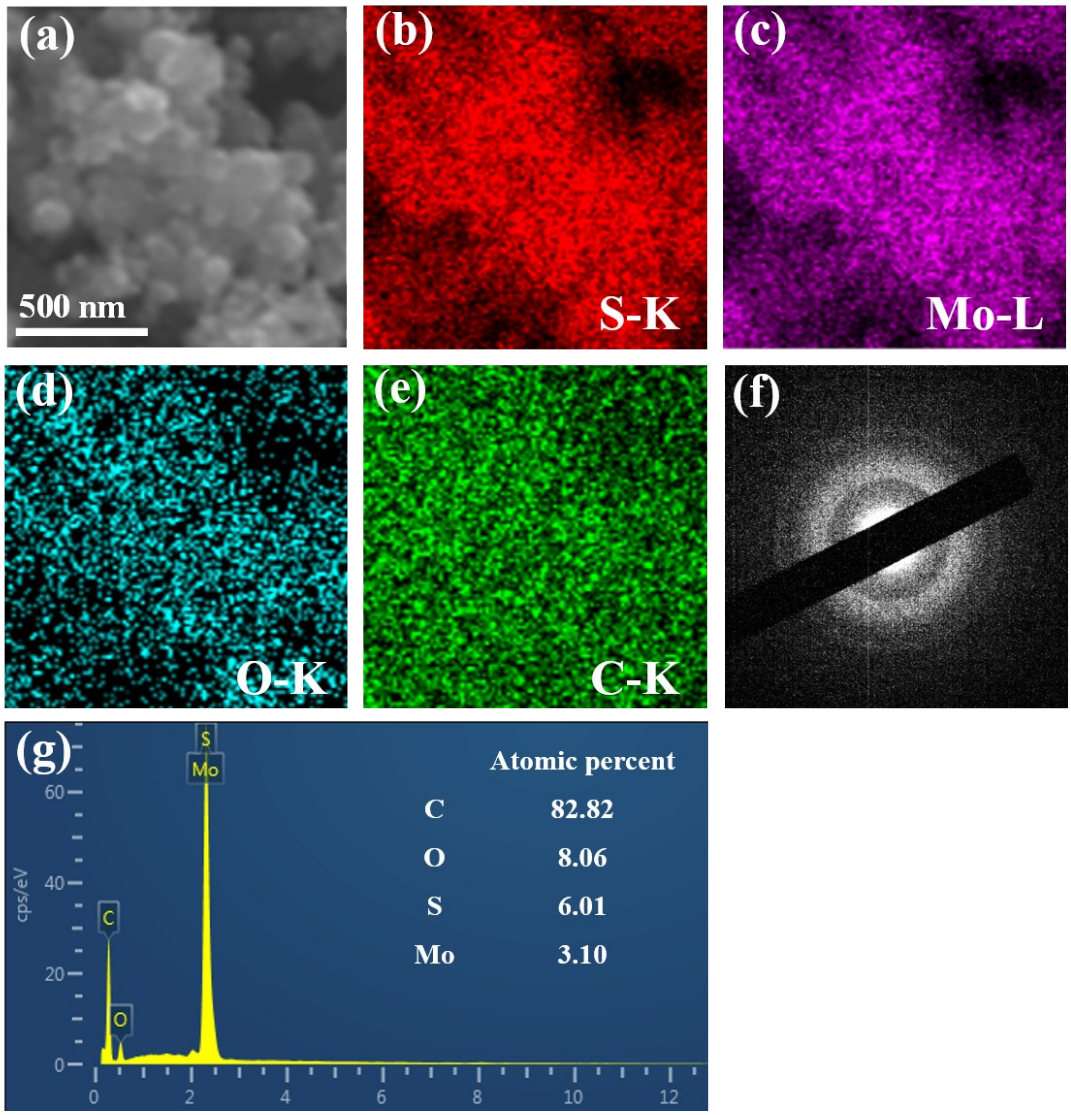

Fig. S2 (a) SEM, (b,c,d,e) corresponding EDX elemental mapping images, (f) SAED pattern and (g) elemental distributions spectrum of MoS_2-p.

The image of C element was inaccurate due to the use of carbon conductive adhesive.

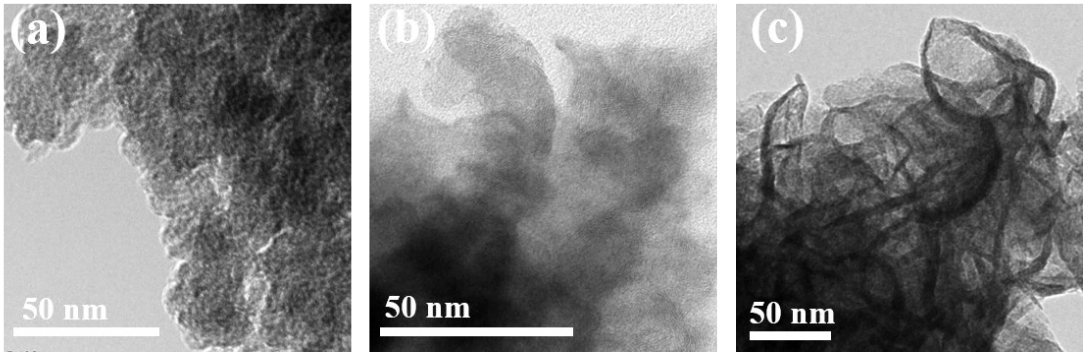

Fig. S3 TEM images of (a) MoS_2-p, (b) MoS_2-m and (c) MoS_2-s.

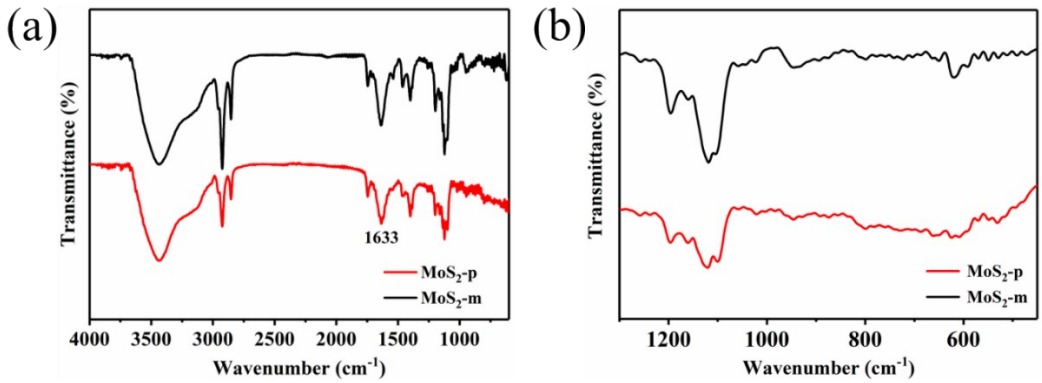

Fig. S4 (a) FTIR spectra and (b) fingerprint region spectra of MoS_2-p and MoS_2-m

The characteristic peak of multi-sulfur bond was not obvious in IR. The presence of the vibration bonds (C=O) at 1633 cm^{-1} suggested the existence of DMF in both MoS_2-p and MoS_2-m. The weak intensity of the vibration was due to the low content of DMF, which was consistent with previous reports.[4] DIB had strong vibration peak at 810~750 $cm^{-1}$and middle vibration peak at 725~680 cm^{-1}. But these peaks were not found, indicating that the polysulfide was degraded in the solvothermal process and the residue DIB unit was washed off in the later stage.

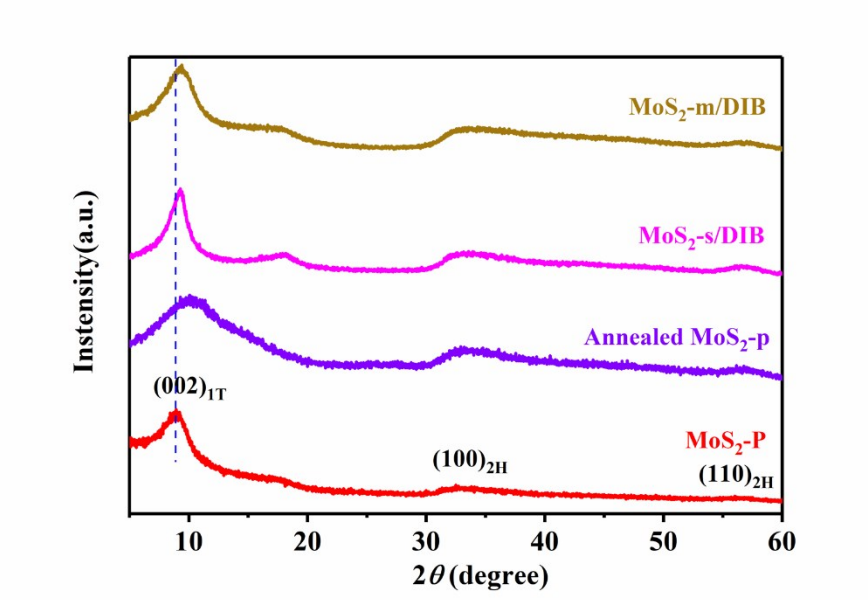

Fig. S5 The XRD pattern of MoS_2-p, Annealed MoS_2-p, MoS_2-s/ DIB, and MoS_2-m/DIB.

MoS_2-p was annealed at 200 °C in Ar atmosphere for 3 h.[5] From the Figure S5, the peak $(002)_{1T}$ of the annealed MoS_2-p shifted to 10.1°, and the intensity of the peak $(100)_{2H}$ and $(110)_{2H}$ was enhanced, which were attributed to partial removal of water bilayer and conversion of 1T phase to stable 2H phase.[6] MoS_2-s/DIB and MoS_2-m/DIB were prepared by using thiourea and sulfur sublimed as the respective sulfur source with extra addition of DIB. XRD diffraction revealed that adding DIB has no effect on the synthesis of MoS_2, indicating that it is necessary that DIB has to be incorporated into the polysulfide in light of the *in situ* exfoliation.

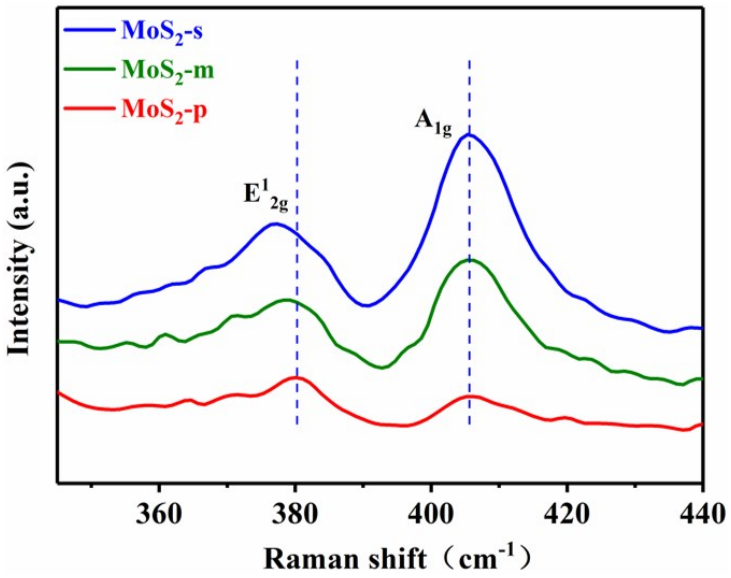

Fig. S6 The Raman spectra of MoS_2-p, MoS_2-m, MoS_2-s.

The enlarged peak width at half-height of both E^1_{2g} and A^1_g peaks (9~11 cm^{-1}), compared to that exfoliated mechanically (2~6 cm^{-1}),[7] implied the inhomogeneity of stack thickness.

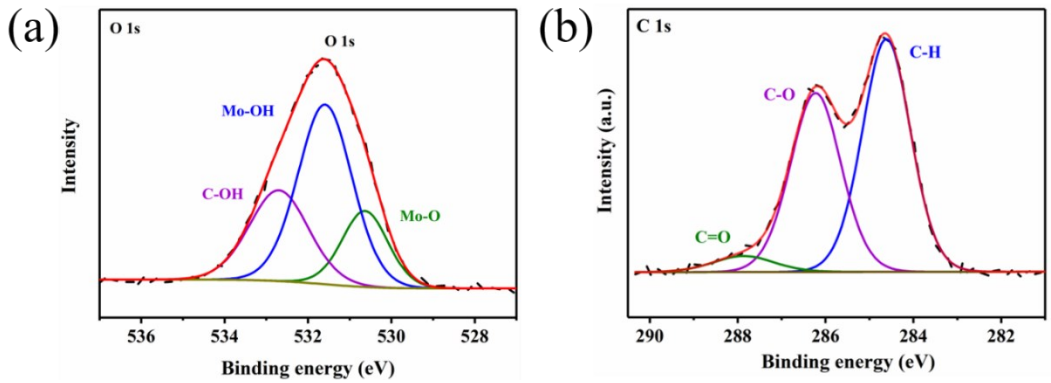

Fig. S7 High resolution XPS spectra of (a) O 1s and (b) C 1s in MoS_2-p.

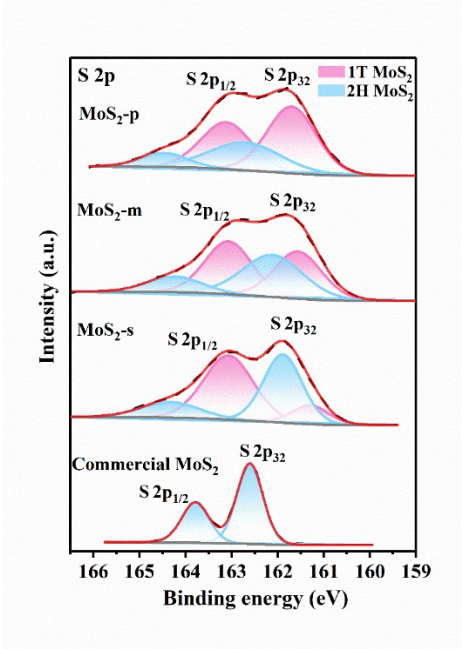

Fig. S9 High resolution XPS spectra of S 2p in MoS_2-p, MoS_2-m, MoS_2-s and commercial MoS_2

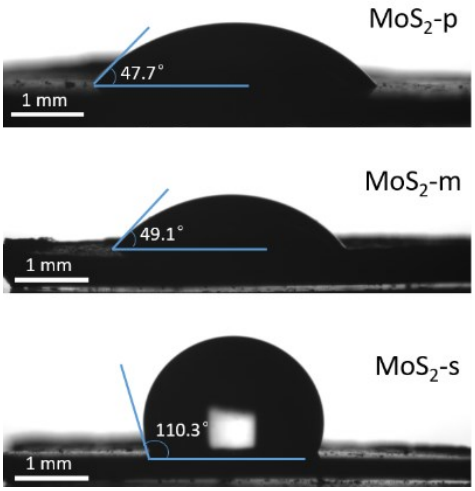

Fig. S10 Contact angle test results of the MoS_2-p, MoS_2-m and MoS_2-T.

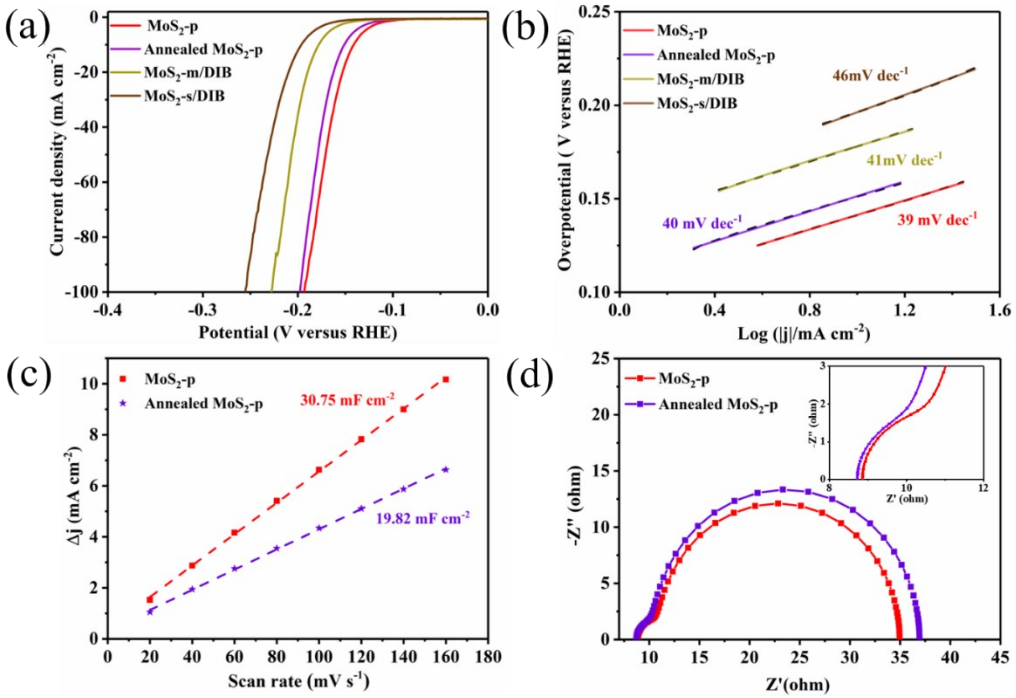

Fig. S11 (a) The polarization curves for MoS_2-p, annealed MoS_2-p, MoS_2-s/DIB and MoS_2-m/DIB with IR compensation. (b) The corresponding Tafel plots derived from the polarization curves. (c)The C_{dl} estimation linear regression and (d) EIS for MoS_2-p and annealed MoS_2-p.

The overpotential at the current density of 10 mA cm^{-2} for annealed MoS_2-p, MoS_2-m/DIB, and MoS_2-s/DIB was 151, 178, and 196 mV, respectively. From the polarization curves (Fig. S9a) and the corresponding Tafel plots (Fig. S9b), the HER performance difference of MoS_2-s (Fig. 4) and MoS_2-s/DIB was not significant. As the removal of water bilayer and 1T phase partial transformation to the 2H phase,[5] the HER performance of annealed MoS_2-p was slightly reduced. The HER process of the MoS_2-p, MoS_2-m, MoS_2-s/DIB, MoS_2-m/DIB and MoS_2-s might be considered as a Volmer-Heyrovsky mechanism, suggesting that electrochemical desorption is the rate-limiting step.[8] Compared with the MoS_2-p, the C_{dl} of annealed MoS_2-p was lower and the R_{ct} (28.2 Ω) was higher (Fig. S9d). This can be due to MoS_2 partial transformation of 1T phase into 2H phase.

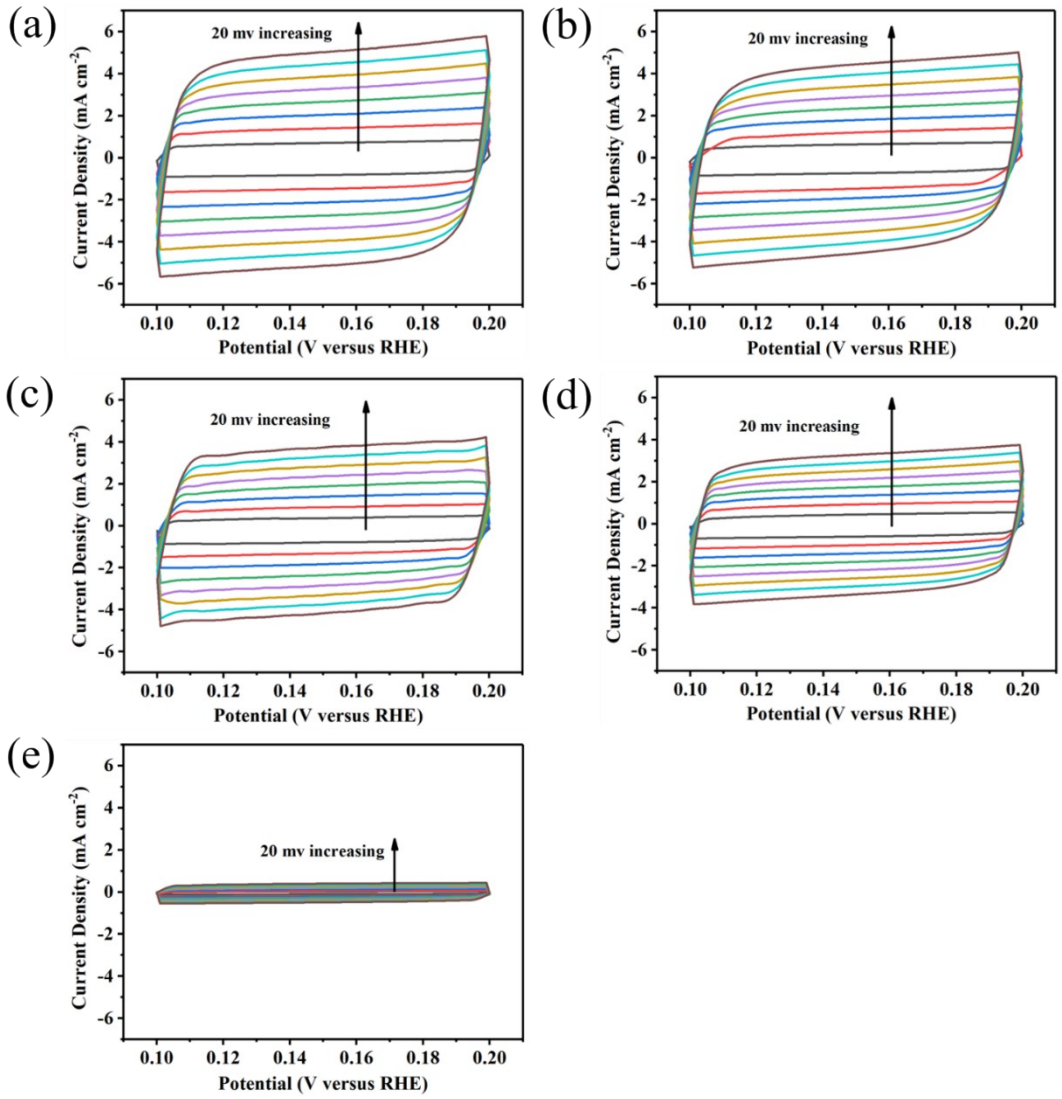

Fig. S12 HER cyclic voltammetry at the scan rates of 20, 40, 60, 80, 100, 120,140 and 160 mV s^{-1} for ECSA of (a) MoS_2-p, (b) MoS_2-m, (c) MoS_2-s, (d) Annealed MoS_2-p and (e) Commercial MoS_2 in 0.1 to 0.2 V vs. RHE range.

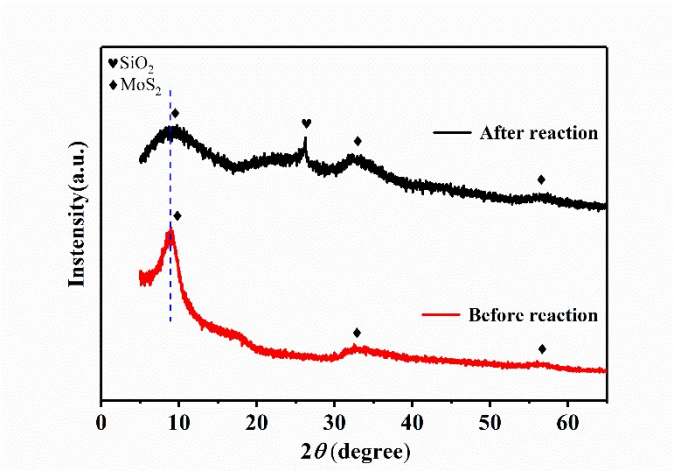

Fig. S13 XRD patterns of MoS_2-p before and after stability test.

XRD patterns of MoS_2-p before and after stability test indicated that the main ingredients after electrolysis were still MoS_2 with enlarged interlayer. The after reaction samples was obtained by dropping MoS_2-p onto carbon paper to electrochemical stability test and then by ultrasound and drying. Since the sample after reaction had a little amount obtained by ultrasound, there was a series of peaks of the glass substrate (26.2°) and cabron (around 23° and 43°) in the after reaction sample. The weak XRD signal suggested the MoS_2-p underwent amorphization during the stability test.

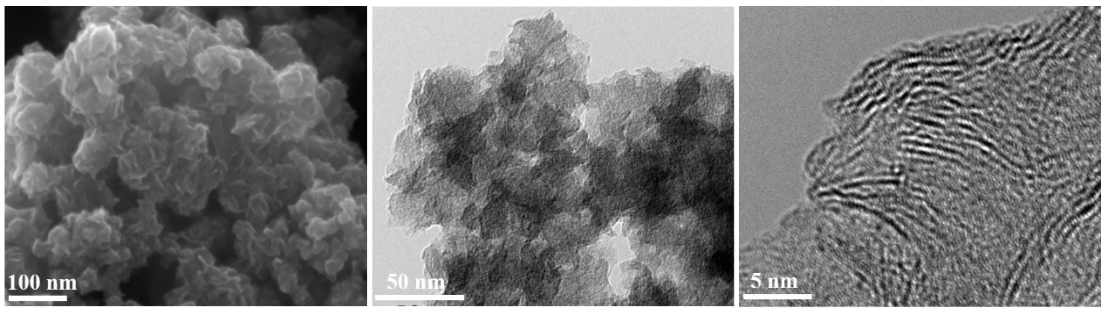

Fig. S14 SEM and TEM of MoS_2-p after stability test.

Table S1 Comparison of HER activity for MoS_2-p with other MoS_2 in acidic media of 0.5 $_M$ H_2SO_4.

Samples	η_{10} [mV]	η_{20} [mV]	η_{100} [mV]	Tafel Slope [mV dec^{-1}]	iR compensation	Reference
Few-layer and 1T-rich MoS_2	141	153	193	39	Yes	This work
Single-crystal MoS_2 nanobelts		170		70	Yes	*ACS Nano*, 2015, 9, 6, 6478[9]
Strained 2H-MoS_2 monolayer	170			60	No	*Nature materials*, 2016, 15, 364[10]
Mesoporous 1T Phase MoS_2 Nanosheets	153			43	Yes	*Journal of The American Chemical Society*. 2016, 138, 7965[11]
1T Phase MoS_2 Nanosheets	203			48	Yes	*Journal of The American Chemical Society*. 2016, 138, 7965[11]
Monolayer MoS_2	>150		>300	50	Yes	*Nature Materials,* 2016, 15, 1003[12]
Amorphous $MoS_{1.7}$	143			39.5	No	*Small,* 2016, 12, 5530[13]
Metallic 1T MoS_2	175			41	No	*Nature Communications*. 2016, 7, 10672[14]
Multiphasic 1T/2H MoS_2	234			46	No	*Journal of Materials Chemistry A*, 2017, 5, 2681[15]
Chemically exfoliated and structurally deformed MoS_2	191		>300	64	Yes	*Advanced Materials*. 2017,29,1703863[16]
High-Percentage (70%) 1T-Phase MoS_2	173			53	Yes	*Advanced Materials*. 2018, 30, 1705509[17]
MoS_2 nanomesh with holes and lattice defects	160			46	Yes	*Applied Catalysis B: Environmental*. 2018, 239,537[18]
Multilayer MoS_2	178			48	Yes	*ACS Sustainable Chemistry & Engineering*. 2019, 7, 6999[19]
MoS_2 quantum dots	256			93	No	*The Journal of*

and pore-rich monolayer MoS_2						*Physical Chemistry Letters*. 2019, 10, 4763[20]
Monomeric MoS_4^{2-}	167			46	Yes	*ACS Catalysis*.2019, 10, 1, 652[21]
Atomic vacancy layered MoS_2	200			65	Yes	*Electrochimica Acta* ,2020, 336, 135740[22]
S-vacancy MoS_2 Nanosheet Arrays on carbon cloth	131			48	Yes	*Journal of The American Chemical Society*. 2020, *142* (9), 4298[23]

References

1. W. J. Chung, J. J. Griebel, E. T. Kim, H. Yoon, A. G. Simmonds, H. J. Ji, P. T. Dirlam, R. S. Glass, J. J. Wie, N. A. Nguyen, B. W. Guralnick, J. Park, A. Somogyi, P. Theato, M. E. Mackay, Y. E. Sung, K. Char and J. Pyun, *Nat. Chem.*, 2013, **5**, 518-524
2. M. K. Salman, B. Karabay, L. C. Karabay and A. Cihaner, *J. Appl. Polym. Sci.,* 2016, **133**.43655
3. F. Cataldo, *Angew. Makromol. Chem.*1997, **249**, 137-149
4. M. R. Gao, M. K. Chan and Y. Sun, *Nat. Commun.,* 2015, **6**, 7493.
5. G. Eda, H. Yamaguchi, D. Voiry, T. Fujita, M. Chen and M. Chhowalla, *Nano Lett.* 2011, **11**, 5111-5116.
6. A. Sellam, R. N. Jenjeti and S. Sampath, *J. Phys. Chem. C,* 2018, **122**, 14186-14194.
7. C. Lee, H. Yan, L. E. Brus, T. F. Heinz, J. Hone and S. Pyu, *ACS Nano,* 2010, **4**, 2695-2700.
8. X. Wang, J. Wang, X. Zhang, Q. Tian, M. Liu, N. Cai, Y. Xue, W. Chen, W. Li and F. Yu, *ChemCatChem,* 2019, **11**, 1354-1361.
9. L. Yang, H. Hong, Q. Fu, Y. Huang, J. Zhang, X. Cui, Z. Fan, K. Liu and B. Xiang, *ACS Nano,* 2015, **9**, 6478-6483.
10. H. Li, C. Tsai, A. L. Koh, L. Cai, A. W. Contryman, A. H. Fragapane, J. Zhao, H. S. Han, H. C. Manoharan, F. Abild-Pedersen, J. K. Norskov and X. Zheng, *Nat. Mater.,* 2016, **15**, 364.
11. Y. Yin, J. Han, Y. Zhang, X. Zhang, P. Xu, Q. Yuan, L. Samad, X. Wang, Y. Wang, Z. Zhang, P. Zhang, X. Cao, B. Song and S. Jin, *J. Am. Chem. Soc.,* 2016, **138**, 7965-7972.
12. D. Voiry, R. Fullon, J. Yang, E. S. C. de Carvalho Castro, R. Kappera, I. Bozkurt, D. Kaplan, M. J. Lagos, P. E. Batson, G. Gupta, A. D. Mohite, L. Dong, D. Er, V. B. Shenoy, T. Asefa and M. Chhowalla, *Nat. Mater.,* 2016, **15**, 1003-1009.
13. A. Y. Lu, X. Yang, C. C. Tseng, S. Min, S. H. Lin, C. L. Hsu, H. Li, H. Idriss, J. L. Kuo, K. W. Huang and L. J. Li, *Small,* 2016, **12**, 5530-5537.
14. X. Geng, W. Sun, W. Wu, B. Chen, A. Al-Hilo, M. Benamara, H. Zhu, F. Watanabe, J. Cui and T. P. Chen, *Nat. Commun.,* 2016, **7**, 10672.
15. D. Wang, X. Zhang, S. Bao, Z. Zhang, H. Fei and Z. Wu, *J. Mater. Chem. A,* 2017, **5**, 2681-2688.
16. Y. C. Chen, A. Y. Lu, P. Lu, X. Yang, C. M. Jiang, M. Mariano, B. Kaehr, O. Lin, A. Taylor, I. D. Sharp, L. J. Li, S. S. Chou and V. Tung, *Adv. Mater.,* 2017, **29**, 1703863.
17. C. Tan, Z. Luo, A. Chaturvedi, Y. Cai, Y. Du, Y. Gong, Y. Huang, Z. Lai, X. Zhang, L. Zheng, X. Qi, M. H. Goh, J. Wang, S. Han, X. J. Wu, L. Gu, C. Kloc and H. Zhang, *Adv. Mater.,* 2018, **30**,1705509
18. Y. Li, K. Yin, L. Wang, X. Lu, Y. Zhang, Y. Liu, D. Yan, Y. Song and S. Luo, *Appl. Catal. B Environ.,* 2018, **239**, 537-544.
19. C. Meng, M.C. Lin, X.W. Du and Y. Zhou, *ACS Sustainable Chem. Eng.* 2019, **7**, 6999-7003.
20. C. Hu, Z. Jiang, W. Zhou, M. Guo, T. Yu, X. Luo and C. Yuan, *J. Phys. Chem.*

Lett., 2019, **10**, 4763-4768.
21. B. Seo, G. Y. Jung, S. J. Lee, D. S. Baek, Y. J. Sa, H. W. Ban, J. S. Son, K. Park, S. K. Kwak and S. H. Joo, *ACS Cat.,* 2019, **10**, 652-662.
22. C. Wang, H. Lu, K. Tang, Z. Mao, Q. Li, X. Wang and C. Yan, *Electrochim. Acta,* 2020, **336**.135740.
23. X. Wang, Y. Zhang, H. Si, Q. Zhang, J. Wu, L. Gao, X. Wei, Y. Sun, Q. Liao, Z. Zhang, K. Ammarah, L. Gu, Z. Kang and Y. Zhang, *J. Am. Chem. Soc.,* 2020, **142**, 4298-4308.